Diode-pumped Yb:CaF 2 multipass amplifier producing 50 mJ with dynamic analysis for high repetition rate operation

Florence Friebel, Alain Pellegrina, Dimitrios N. Papadopoulos, Patrice Camy, Jean-Louis Doualan, Richard Moncorgé, Patrick Georges, Frédéric Druon

Diode-pumped Yb:CaF2 multipass amplifier producing 50 mJ with dynamic analysis for high repetition rate operation

Florence Friebel[1], Alain Pellegrina[2], Dimitris N. Papadopoulos[2], Patrice Camy[3], Jean-Louis Doualan[3], Richard Moncorge[3], Patrick Georges[1], Frédéric Druon[1]

[1]*Laboratoire Charles Fabry, Institut d'Optique, CNRS, Univ Paris Sud 11, 2 Av. A. Fresnel, 91127 Palaiseau Cedex, France*
[2]*Laboratoire d'Utilisation des Lasers Intenses, CNRS, Ecole Polytechnique, CEA, Univ P. et M. Curie, Palaiseau, France*
[3]*Centre de Recherche sur les Ions, les Matériaux et la Photonique, CNRS, CEA, ENSI Caen, Université de Caen, France*
*Florence.Friebel@ institutoptique.fr

Abstract The dynamic thermal issues of the Yb:CaF_2 crystals within a multi-tens-mJ-energy multipass amplifier operating in the 20–100 Hz repetition rate range and pumped in quasi-cw regime have been studied at different timescales. Thermal response times of the system have been precisely investigated and analyzed, for the first time to our best knowledge in such amplifiers. This study includes a dual timescale analysis: in the long-time-scale (second) with direct thermography mapping and in the millisecond range with thermal lensing in a pump-probe configuration. Very atypical positive lens behavior with fluorites will also be presented and discussed. This complete analysis is used to demonstrate the capability of Yb:CaF_2 multipass amplifier systems for operating the amplifier at 20 Hz with 57 mJ and 100 Hz with 32-mJ stable regime. Indeed, high repetition rate multipass amplifier has been realized for the first time with Yb:CaF_2 and for this energy. The results have been analyzed precisely to take into account the thermal issues and excellent beam quality, with a M_2 of 1.1. The pointing stability of 20 lrad has been measured documenting the reliability of the high repetition rate mJ amplifier.

1 Introduction

The interest in diode-pumped solid-state lasers is more than ever growing, especially since the development of many large-scale high-energy ''high repetition rate'' laser facilities. For these large-scale installations, cost-efficient solutions are preferred. Efficient diode pumping usually involves ytterbium-doped materials [1–16]. The development of the technology is mainly based on the knowledge of the amplifying material. Among the interesting ytterbium-doped materials, Yb:CaF_2 is interesting for a number of attractive properties [3, 6, 7, 13, 15]. It possesses a longfluorescence
lifetime, 2.4 ms, which facilitates the storage of energy [4]. Also, the large bandwidth of this material makes it an attractive candidate for the generation and amplification of ultrashort pulses [5, 11, 12, 15, 17–19]. The material also sustains high average power thanks to its good thermal conductivity, 6 $Wm_{-1} K_{-1}$ (for a typical doping of 2%) [13, 14, 20]. Thermal and spectroscopic parameters suggest Yb-doped materials and in particular Yb:CaF_2 to be a good choice for diode-pumped high-power lasers. In the frame of the Cilex-Apollon 10PW project, we are developing new OPCPA pump sources based on those crystals [21]. Yb:CaF_2 performances and specifics are the subject of the current article. The Yb:CaF2 can be used for high-energy and high-power amplifiers. The challenges occur when working at high power. This automatically implies heat dissipation that may lead to thermo-optical distortions on the crystal [22–25]. Moreover, in highenergy lasers, the pumping is often accomplished in quasicw regime, which leads to an unsteady state and a dynamic of these phenomena. In this paper, we investigate experimentally for the first time, to our knowledge, this dynamic for an Yb-doped material. To apprehend this dynamic, the crystal is investigated on its in situ opto-mechanical, setup.
Based on these experiments, we subsequently design a multipass amplifier able to generate 50-mJ pulse at high repetition rate (for this kind of systems): 20–100 Hz.

2 Amplifier setup

The experiment was performed on a multipass amplifier composed of two Yb:CaF2 crystals: 2-mm-thick and 15-mm-diameter and doped at 2.2 %, in an active-mirror configuration (Fig. 1). The ytterbium-doped material is pumped from the front side. Those disks are glued to a copper mounts that supports water-cooling from the backside. The cooling temperature is set to 13 □C. The pump diode emits 400 W peak power at 980 nm with 1–3 ms pulses in quasi-cw operation, with a repetition rate typically between 20 and 100 Hz. The diode is fiber coupled using a 400 lm diameter NA ¼ 0:22 fiber. The pump beam is imaged through a telescope (f ¼ 80 mm, f ¼ 250 mm) to a pump beam diameter of 1.5 mm. The pump energy is in the joule range and the average pump power in the 100 W range. The first crystal absorbed 33.5 % and the remained pumped is re-imaged on the second crystal using 2f–2f configuration with a 150-mm lens. After the second crystal, 60.9 % of the total pump energy is absorbed. The target energy range of this amplifier is 50 mJ with a gain of 50. To reach this gain, multiple passes (typ. 18) have to be done due to the relatively low gain of Yb:CaF2. The thermal lenses of the crystals are then accumulated numerous times. Moreover, since the amplifier operates close to the damage threshold of the Yb:CaF2 coatings, the beam size signal evolution occurring during the multiple passes is very critical and so is the knowledge to compensate the thermal lens. This implies a good knowledge of the thermal behavior of our laser heads.

3 Slow dynamic study using thermography

We thus perform experiments to have precise values of the thermal effects occurring in the laser head (Fig. 2). With our setup, we can visualize the temperature at the front side

of the crystal using a thermal camera and measure the thermal dynamic of the system in the second timescale. To access to the thermo-optic behavior at the millisecond timescale, we use a nanosecond signal pulse in a pumpprobe configuration by adjusting the delay and monitoring the thermal wavefront distortion (cf. Sect. 4). The experiment has been carried out at 20 and 100 Hz.

First, we investigated the surface temperature of the crystal with a thermal camera operating in the 8–12 lm range, which allows access to the slow dynamic of the heating of the crystal. The temporal behavior is the same in the center and at the edge of the crystal (Fig. 3), indicating a link to the global heating of the crystal [3, 18, 22]. The maximum increase in temperature is only 15 □C at 100 Hz for 2.25-ms pulses with a corresponding average absorbed power of 33.5 W. The profile of temperature is given in Fig. 3 (lower left). The thermal dynamic measurements give a slow rise and fall time, it is 4.6 s at 100 Hz and 3.3 s at 20 Hz. In conclusion, our cooling geometry allows handling efficiently the heating of the crystal avoiding too high-temperature spatiotemporal gradients.

4 Fast thermal dynamic study using thermal lens measurements

The next step includes the observation of the thermal lens established by the spatiotemporal gradient. For this, we used a Shack–Hartmann wavefront analyzer. The crystal is probed by 1030-nm, 1.5-mm-diameter beam (corresponding to the seed signal). This beam makes one bounce in the crystal and is imaged in the wavefront sensor with a 1:1 ratio. The thermal wavefront deformation is isolated by subtracting the static wavefront (without pumping) [20, 26]. As expected with increasing absorbed pump power, the dioptric power is increasing proportionally in absence of saturation (Fig. 4). The thermo-optic coefficient gives a positive value of v ¼ 2 □ 10□6K□1; which may seem counterintuitive taking into account only the different parameters for CaF2 crystal from the literature [22, 27, 28]. The strong effect of the overall mechanical distortion clearly appears, which implies a strong influence of the global design. There is a mixing of thermal lens (negative lens), and thermal disc deformation (positive lens). This is due to the crystal's geometry where the temperature evolution follows a transversal and longitudinal heat distribution over time. The different coatings, the glue, and the design of the copper mount play also an important role. This positive thermal lens has to be considered in the multipass setup (Fig. 1).

In order to be more precise in the thermal-lens-compensation and on using the ns probe, the thermal lens dynamics around its mean value is also studied. With the results obtained, here, we aim to set the optimal correction for the thermal lens occurring at the extraction instant, id est, when the stored energy is at maximum in the gain medium. The measurements reported in the Figs. 5, 6, 7 were performed for 2.25 ms and 400 W peak-power pump pulses at 100 or 20 Hz repetition rates (which corresponds, respectively, to 90 W and 18 W in average power). The probe beam has the same characteristics as above with a pulse duration of 1.5 ns. The thermal lens dynamics are visualized together with the pump pulse end the fluorescence transient (Figs. 5, 6, 8). In our case, the dioptric powers of the thermal lenses are relatively low and their variation versus time even lower. This sensitivity has been indicated with error bar in the graphs. The error bars correspond to the minimum dioptric power measurable with our setup; it has been characterized experimentally measuring the dioptric power variation around a static value. It depends on the parasitic light and on the integration time of the sensor. What we clearly observe is that the maximum of the dioptric power (blue curve) does not correspond to the end of the pump pulse pump—where the laser probe pulse is supposed to be launched to extract the stored energy. Indeed, the maximum occurs 2 ms after the end of the pump pulse. To understand this delay, we numerically calculate using Comsol the temperature dynamics in the crystal assuming a heat load with a shape proportional to the shape of the pump pulse (red curve) or to the shape of the fluorescence transient (purple curve). In all the numerical simulations, only the backside surface is cooled, and the heat is homogeneously deposited with a total average power corresponding to the fractional thermal loads id est 5 % of the absorbed pump power [28]. The derived temperature evolutions are presented: The black curve corresponds to a thermal-load shape similar to the pump pulse in Fig. 6 and the green curve similar to the fluorescence one in Figs. 6, 8. These calculations clearly indicate that fluorescence causes the delay. Indeed, the heat load is linked to the fluorescence in this quasi-3-level laser system and not to the pump pulse. If the main contribution comes from the quantum defect—which is likely the case for a system like Yb:CaF2 [22, 28] whose quantum efficiency is very close to 1—the heat load occurs only after desexcitation of the Yb3þ ions, id est, after fluorescence or laser effect. This delay in the heat load can thus explain the delay between the maximum thermal distortion and the end of the pump pulse. At 100 Hz, however, the amplitude of the thermal variation remains relatively small within about 4 % around the mean value. But, repeating the experiment at 20 Hz, as shown in Fig. 7, the amplitude of the thermal lens variation rises up to about □35 % below and above the mean value. Indeed, these amplitude variations can be seen as a low-pass-filter response, with a cutoff time of 35 ms. This is far from negligible: The maximum lens dioptry can be largely higher than the one really seen by the pulses at the extraction time in qcw sub-100-Hz amplifiers. Moreover, this marks also a strong difference between the quasi-3-level nature of Yb-doped crystals pumped at 980 nm, such as Yb:CaF2, and the quasi-4-level crystals such as Yb:YAG pumped at 940 nm. In the case of zero-line pumping, the mean thermal lens value corresponds fairly to the thermal lens seen by the amplified signal, whereas in a quasi-4-level scheme, the thermal lens seen by the signal is much closer to its maximum since the heat load partly occurs also when the pump is absorbed.

5 Amplifier results

The exact knowledge of the thermal evolution in the active mirrors heads in qcw regime allows us to realize an optimal amplifier design. The multipass cavity setup is shown in Fig. 1. For the seed, in the Cilex-Apollon 10 PW project, the 1030-nm-signal beam is generated by the leak of a Ti:Sapphire oscillator. It is then amplified in a fiber amplifier and stretched to 1.5 ns, and finally further amplified in a Yb:KYW regenerative amplifier (S-pulse HR from Amplitude Systems). The input signal of the Yb:CaF2 multipass amplifier consists in 1.5-ns, 3.1-nm-bandwidth stretched pulses at 1 kHz with an energy of 1.1 mJ at 1030 nm. The multipass amplifier is based on a re-imaging

configuration using two 2-m radius of curvature (ROC) mirrors. It allows easily obtaining nine bounces on each crystal. In order to double the number of passes, a reinjection configuration with a f ¼ 500 mm lens, a quarterwaveplate, and a mirror is added.

To compensate the thermal lens of the crystals, the center mirror of the amplifier (Mth, Fig. 1) can be moved: backward for a negative thermal lens and forward for positive thermal lens. In the optimal configuration, at 20 Hz, the energy output of this amplifier is 57 mJ for 0.89 J of diode pump energy corresponding to an optical to optical efficiency of 6.4 %. The operation has been longterm stable with a pointing stability of 20 lrad over 30 min. The beam profile is excellent with a M2 ¼ 1:1 (Fig. 9). The gain is then 52 for 18 passes. Unfortunately, the strong bias of Yb:CaF2 to fluoresce becomes a critical issue at 100 Hz. Indeed, a strong amount of non-extracted energy is dispersed into fluorescence. In our setup, this fluorescence hits the mounts in close vicinity of the active medium. This creates, at high repetition rate, air turbulences and fluctuations in the laser beam. In order to avoid stability issues, the setup is modified, changing the optics positions to reduce the deleterious heat dissipation on mounts. In this modified setup, 32 mJ have been obtained at 100 Hz (Fig. 9)with beam-pointing stabilities close to the 20 Hz regime and an excellent beam profile similar to the 20 Hz regime. Up to 39 mJ have been obtained with this setup with a good stability during hours. But at this level, erratic damage appears due to the continuous exposure to high energy at high repetition rate. To operate more safely, we decide to decrease the energy down to 30 mJ for the very-long-term operation.

The measured spectrum remains also identical (3.1 nm FWHM, FTL 500 fs) to the injected one (Fig. 10) showing the interest to use Yb:CaF2 gain medium to avoid any gain narrowing [5, 13–15].

6 Conclusion

To summarize, the exact measurement of the thermal lens allows us to optimize the design of the Yb:CaF2 amplifier avoiding beam focusing and then to extract efficiently and reliably the energy without damaging the optics and access safely to a reliable stable regime within a 50-mJ range. This investigation represents, to our knowledge, the first study of the static and dynamic thermal issues of an Ybdoped crystal (namely Yb:CaF2) pumped in qcw regime.

We demonstrated first that a positive thermal lens is possible despite the negative thermo-optic coefficient of CaF2. This counterintuitive result is explained by the geometry of the gain medium: An active-mirror crystal glued to a copper heat-sink. Its deformation due to heat adds to the thermal-lensing effect. Second, we also studied the dynamics of the measured thermal lens at short timescales. A delay between the maximum of the pump pulse and the maximum of the distortion has been observed. This has been linked to the quasi-3-level nature of Yb:CaF2, a result that could be easily generalized to other Yb-doped materials pumped into their zero line. Our precise experimental study has also allowed us to optimize the design of a multipass amplifier based on dual Yb:CaF2 producing 57 mJ at 20 Hz and 32 mJ at 100 Hz (Fig. 9). Such high repetition rate multipass amplifiers can be seen as a compact (the footprint of this amplifier is 80 □ 20 cm2), robust, and simple module to boost commercial Yb-doped mJ laser chains sustaining a broad spectrum while keeping a good quality and stable laser beam.

Acknowledgments This work has been partially supported by the French National Research Agency (ANR) through the Femtocryble program and by the ILE 07-CPER 017-01 contract.

References

1. F. Druon, F. Balembois, P. Georges, New materials for shortpulse amplifiers. IEEE Photonics J. 3(2), 268–273 (2011)
2. J.-C. Chanteloup, D. Albach, A. Lucianetti, K. Ertel, S. Banerjee, P.D. Mason, C. Hernandez-Gomez, J.L. Collier, J. Hein, M. Wolf, J. Ko¨rner, B.J. Le Garrec, Multi kJ level laser concepts for HiPER facility. J. Phys. Conf. Ser. 244(1), 012010 (2010)
3. Fre´de´ric Druon, Sandrine Ricaud, Dimitris N. Papadopoulos, Alain Pellegrina, Patrice Camy, Jean Louis Doualan, Richard Moncorge´, Antoine Courjaud, Eric Mottay, Patrick Georges, On Yb:CaF_2 and Yb:SrF_2: review of spectroscopic and thermal properties and their impact on femtosecond and high power laser performance [invited]. Opt. Mater. Express 1(3), 489–502 (2011)
4. M. Siebold, M. Hornung, S. Bock, J. Hein, M.C. Kaluza, J. Wemans, R. Uecker, Broad-band regenerative laser amplification in ytterbium-doped calcium fluoride (Yb:CaF_2). Appl. Phys. B 89(4), 543–547 (2007)
5. Mathias Siebold, Marco Hornung, Ragnar Boedefeld, Sebastian Podleska, Sandro Klingebiel, Christoph Wandt, Ferenc Krausz, Stefan Karsch, Reinhard Uecker, Axel Jochmann et al., Terawatt diode-pumped Yb:CaF_2 laser. Opt. Lett. 33(23), 2770–2772 (2008)
6. M. Siebold, S. Bock, U. Schramm, B. Xu, J.L. Doualan, P. Camy, R. Moncorge´, Yb:CaF_2—a new old laser crystal. Appl. Phys. B 97(2), 327–338 (2009)
7. Thomas Toepfer, Joerg Neukum, Joachim Hein, Mathias Siebold, Very-large-scale DPSS lasers are coming. Laser Focus World 46(10), 64–67 (2010). WOS:000283682500021
8. Mathias Siebold, Fabian Roeser, Markus Loeser, Daniel Albach, Ulrich Schramm, PEnELOPE: a high peak-power diode-pumped laser system for laser-plasma experiments. Proc. SPIE 8780, 878005–87800514 (2013)
9. Marco Hornung, Sebastian Keppler, Ragnar Bo¨defeld, Alexander Kessler, Hartmut Liebetrau, Jo¨rg Ko¨rner, Marco Hellwing, Frank Schorcht, Oliver Ja¨ckel, Alexander Sa¨vert, Jens Polz, Ajay Kawshik Arunachalam, Joachim Hein, Malte C. Kaluza, Highintensity, high-contrast laser pulses generated from the fully diode-pumped Yb:glass laser system POLARIS. Opt. Lett. 38(5), 718–720 (2013)
10. Alexander Kessler, Marco Hornung, Sebastian Keppler, Frank Schorcht, Marco Hellwing, Hartmut Liebetrau, Jo¨rg Ko¨rner, Alexander Sa¨vert, Mathias Siebold, Matthias Schnepp, 16.6 J chirped femtosecond laser pulses from a diode-pumped Yb:CaF_2 amplifier. Opt. Lett. 39(6), 1333–1336 (2014)
11. G. Machinet, P. Sevillano, F. Guichard, R. Dubrasquet, P. Camy, J.-L. Doualan, R. Moncorge´, P. Georges, F. Druon, D. Descamps, E. Cormier, High-brightness fiber laser-pumped 68W Kerr-lens mode-locked Yb:CaF_2 oscillator. Opt. Lett. 38(20), 4008–4010 (2013)
12. P. Sevillano, G. Machinet, R. Dubrasquet, P. Camy, J-L. Doualan, R. Moncorge, P. Georges, F.P. Druon, D. Descamps, E. Cormier. Sub-50 fs, Kerr-lens mode-locked Yb:CaF_2 laser oscillator delivering up to 2.7 W. In Advanced Solid-State Lasers Congress, page AF3A.6. Optical Society of America, 2013
13. V. Petit, J.L. Doualan, P. Camy, V. Me´nard, R. Moncorge´, CW and tunable laser operation of Yb_3? doped CaF_2. Appl. Phys. B

78(6), 681–684 (2004)
14. J.L. Doualan, P. Camy, A. Benayad, V. Me´nard, R. Moncorge´, J. Boudeile, F. Druon, F. Balembois, P. Georges, Yb3? doped (Ca, Sr, Ba)F2 for high power laser applications. Laser Phys. 20(2), 533–536 (2010)
15. R. Moncorge´, P. Camy, J.L. Doualan, A. Braud, J. Margerie, L.P. Ramirez, A. Jullien, F. Druon, S. Ricaud, D.N. Papadopoulos et al., Pure and Yb3? doped fluorites (Ca, Sr, Ba)F2: a renewal for the future high intensity laser chains. J. Lumin. 133, 276–281 (2013)
16. T. Balcˇiu¯nas, G.Y. Fan, G. Andriukaitis, A. Pugzˇlys, A. Baltusˇka,
High-power top-hat pulses from a Yb master oscillator power amplifier for efficient optical parametric amplifier pumping. Opt. Lett. 37(13), 2547–2549 (2012)
17. F. Friebel, F. Druon, J. Boudeile, D.N. Papadopoulos, M. Hanna, P. Georges, P. Camy, J.L. Doualan, A. Benayad, R. Moncorge et al., Diode-pumped 99 fs Yb:CaF2 oscillator. Opt. Lett. 34(9), 1474–1476 (2009)
18. P.A. Popov, P.P. Fedorov, V.V. Osiko, Thermal conductivity of single crystals with a fluorite structure: cadmium fluoride. Phys. Solid State 52(3), 504–508 (2010). WOS:000275755200009
19. Sandrine Ricaud, Fre´de´ric Druon, Dimitris N. Papadopoulos, Patrice Camy, Jean-Louis Doualan, Richard Moncorge´, Martin Delaigue, Yoann Zaouter, Antoine Courjaud, Patrick Georges et al., Short-pulse and high-repetition-rate diode-pumped Yb:CaF2 regenerative amplifier. Opt. Lett. 35(14), 2415–2417 (2010)
20. G. Andriukaitis, T. Balciunas, L. Zhu, T. Flo¨ry, A. Verhoef, A. Fernandez, A. Pugzlys, A. Baltuska, M. Grishin, A. Michailovas. Suppression of Population-Lifetime-Determined Energy Instability
in a Femtosecond kHz Yb CPA. In Conference on Lasers and Electro-Optics 2012, page CM1D.5. Optical Society of America. 2012
21. Dimitrios N. Papadopoulos, Alain Pellegrina, Lourdes Patricia Ramirez, Patrick Georges, Fre´de´ric Druon, Broadband highenergy
diode-pumped Yb:KYW multipass amplifier. Opt. Lett. 36(19), 3816–3818 (2011)
22. Sebastien Che´nais, Fre´de´ric Druon, Sebastien Forget, Franc¸ois
Balembois, Patrick Georges, On thermal effects in solid-state lasers: the case of ytterbium-doped materials. Prog. Quantum Electron. 30(4), 89–153 (2006)
23. Sebastien Che´nais, F. Balembois, F. Druon, G. Lucas-Leclin, P. Georges, Thermal lensing in diode-pumped ytterbium lasers-Part I: theoretical analysis and wavefront measurements. IEEE J. Quantum Electron. 40(9), 1217–1234 (2004)
24. S. Che´nais, F. Balembois, F. Druon, G. Lucas-Leclin, P. Georges, Thermal lensing in diode-pumped ytterbium lasers-Part II: evaluation
of quantum efficiencies and thermo-optic coefficients. IEEE J. Quantum Electron. 40(9), 1235–1243 (2004)
25. S. Che´nais, S. Forget, F. Druon, F. Balembois, P. Georges, Direct
and absolute temperature mapping and heat transfer measurements
in diode-end-pumped Yb:YAG. Appl. Phys. B 79(2), 221–224 (2004)
26. A. Pugzˇlys, G. Andriukaitis, D. Sidorov, A. Irshad, A. Baltusˇka, W.J. Lai, P.B. Phua, L. Su, J. Xu, H. Li, R. Li, S. Alisˇauskas, A. Marcinkevicˇius, M.E. Fermann, L. Giniu¯nas, R. Danielius, Spectroscopy and lasing of cryogenically cooled Yb, Na:CaF2. Appl. Phys. B 97(2), 339–350 (2009)
27. Pavel A. Loiko, Konstantin V. Yumashev, Vladimir N. Matrosov, Nikolai V. Kuleshov, Dispersion and anisotropy of thermo-optic coefficients in tetragonal GdYVO4 and YVO4 laser host crystals. Appl. Opt. 52(4), 698 (2013)
28. J. Boudeile, J. Didierjean, P. Camy, J.L. Doualan, A. Benayad, V. Me´nard, R. Moncorge´, F. Druon, F. Balembois, P. Georges, Thermal behaviour of ytterbium-doped fluorite crystals under high power pumping. Opt. Express 16(14), 10098–10109 (2008)

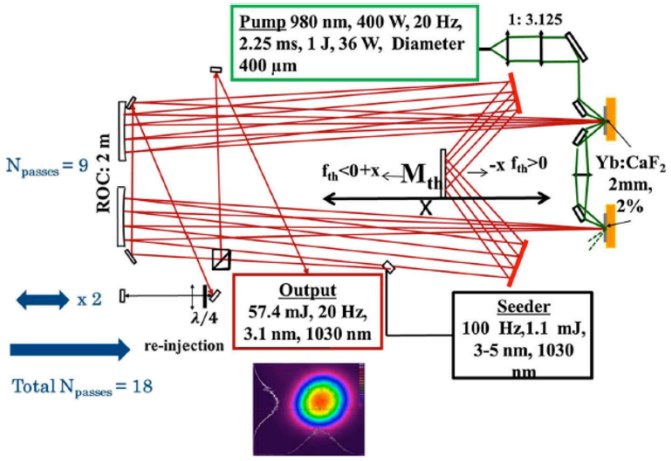

Fig. 1 The multipass amplifier setup. The laser diode pump (*top*) is recycled between the two crystals (*right*). The signal beam is coming from a regenerative amplifier (Seeder, *bottom right*). The signal is represented with only four passes for clarity. The signal is re-injected to double the passes (*bottom left*)

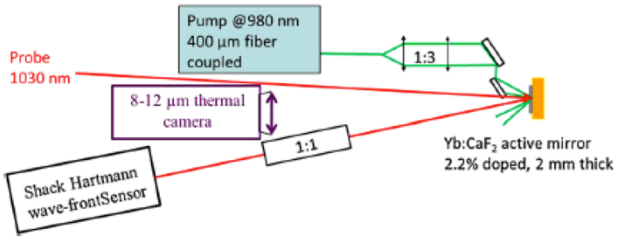

Fig. 2 Dynamic thermal measurements setup of the active mirror in the same pumping configuration than the ones used for the multipass amplifier

Fig. 3 (*left*) Thermal imaging of the crystal and it cross section for 90 W of incident pump (33-W absorbed). The *dynamic* is shown during the switch on and switch off of the diode. (*right*) Displayed in this curve is the point at the center of the crystal measured at 100 Hz (*red curve*) and 20 Hz (*blue curve*)

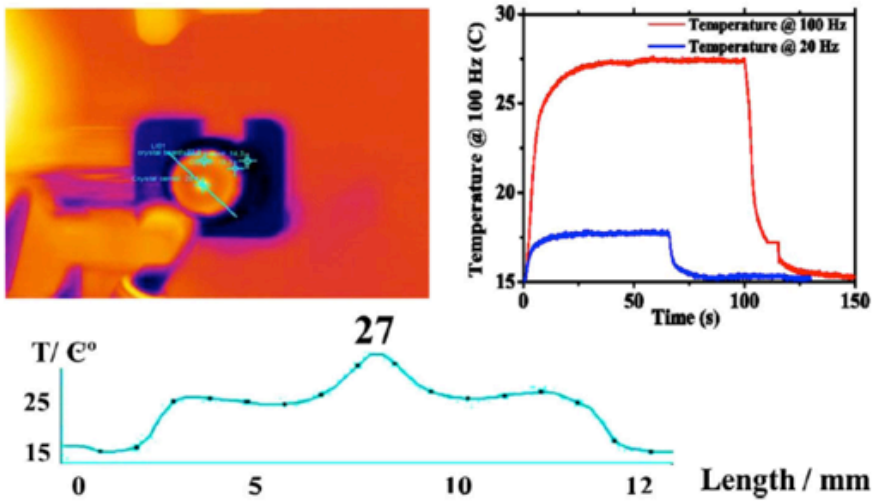

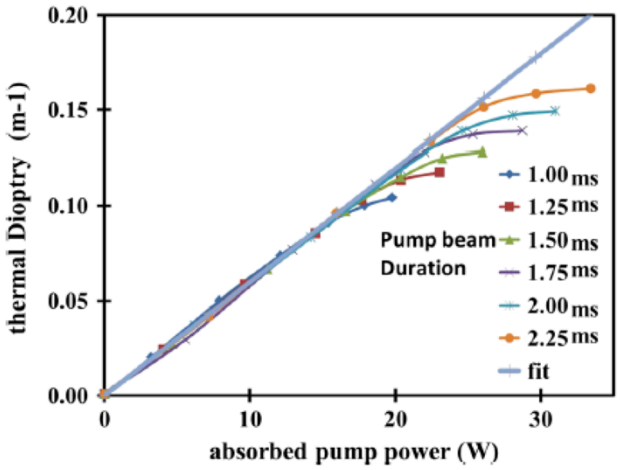

Fig. 4 The average dioptric power plotted versus average absorbed pump power for different pump beam durations (between 1 and 2.25 ms) at 100 Hz

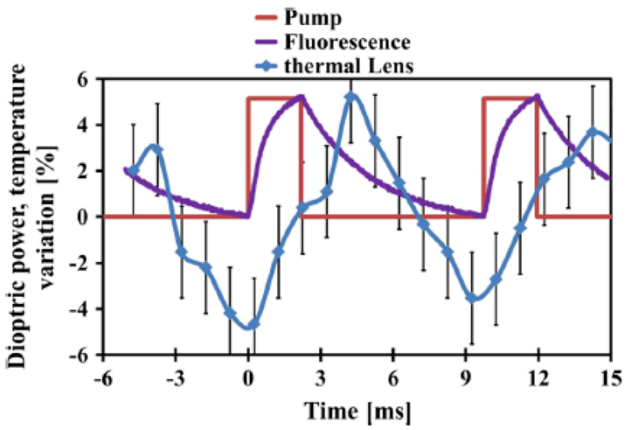

Fig. 5 Measurement of the thermal lens dynamics (*blue curve*) at a 100 Hz repetition rate, given in terms of dioptric variation compared with the mean dioptric power value. Laser pump pulse (*red curve*) and the fluorescence (*purple curve*) transients are also represented

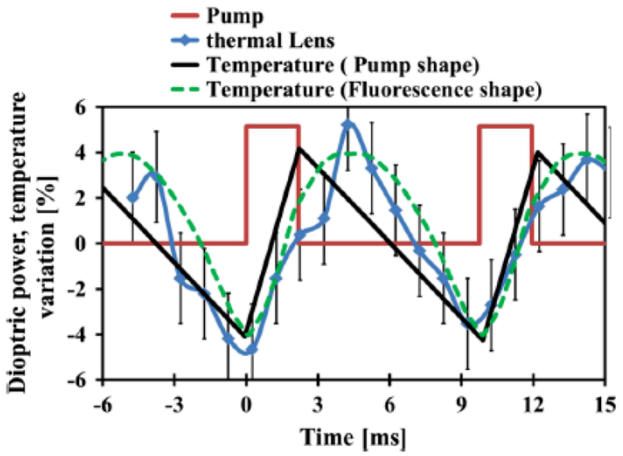

Fig. 6 Measurement of the thermal lens dynamics (*blue curve*) at a 100 Hz repetition rate and comparison to the numerically calculated temperature evolutions of the crystal—also given in terms of variation compared with its mean value—assuming thermal-load shapes as proportional to the shape of the pump pulse (*black curve*) and as to the fluorescence one (*green curve*), (i.e., theoretical temperatures in both cases). The pump pulse is indicated as reference (*red curve*)

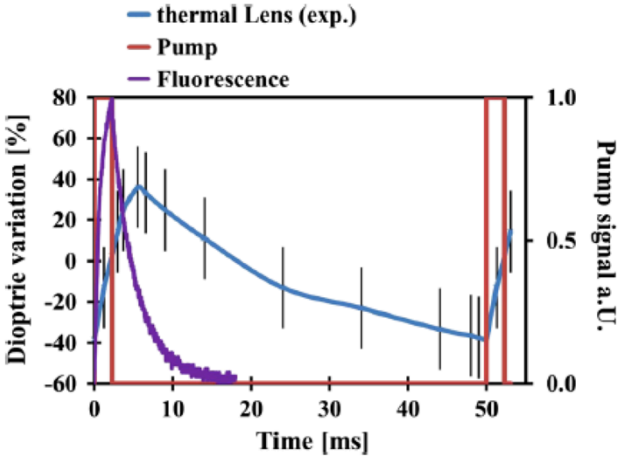

Fig. 7 The graph shows a measurement of the thermal lens dynamics (*blue curve*) at 20-Hz repetition rate on the left side with the fluorescence (*purple curve*) plotted for reference. In the right graph, the numerically calculated temperature evolution of the crystal assuming a thermal-load shape as the fluorescence one (*green curve*) as comparison—both given in terms of variation compared with their mean value. Also, the pump pulse (*red curve*) and fluorescence (*purple curve*) are plotted for reference. Pump pulse and fluorescence are plotted as normalized power over time

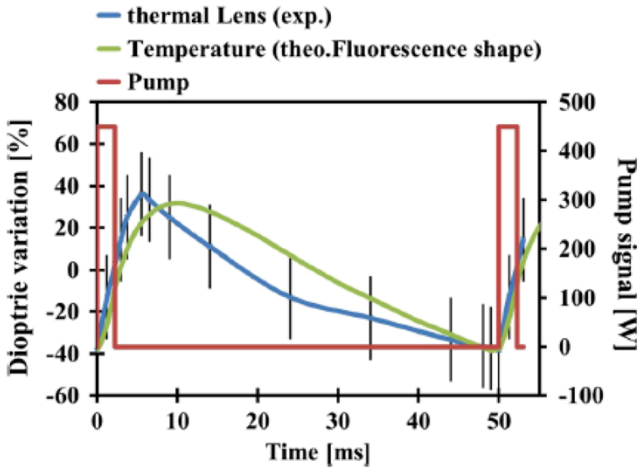

Fig. 8 This figure shows the numerically calculated temperature evolution of the crystal assuming a thermal-load shape as the fluorescence one (*green curve*) as comparison to the thermal lens dynamics (*blue curve*) at 20 Hz—both given in terms of variation compared to their mean value. The pump pulse (*red curve*) is plotted for reference

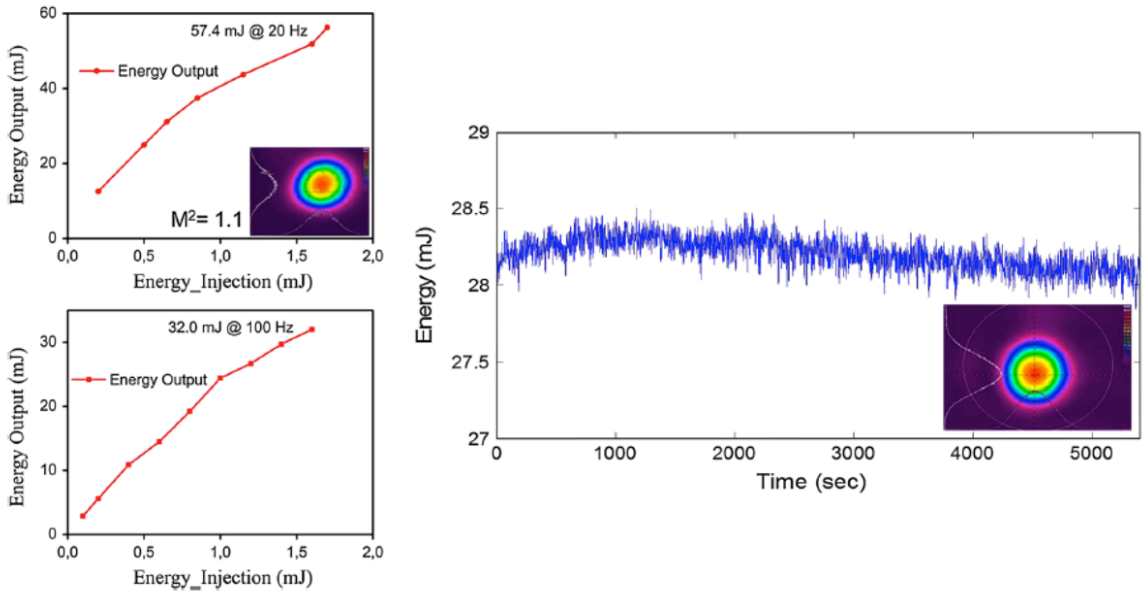

Fig. 9 At 20 Hz, the curve on the *top left side* shows the energy output over injection energy. The maximum output is 57 mJ in the double-passed amplifier. The beam profile is excellent with $M^2 = 1.1$. At 100 Hz (*bottom left side*), the amplifiers delivers 32 mJ extracted Energy. On the right side, we see the peak to peak stabilization over $1\frac{1}{2}$ hours deviates only around 1.7 % over the average output energy and the beam profile (for 32 mJ at 100 Hz) is excellent

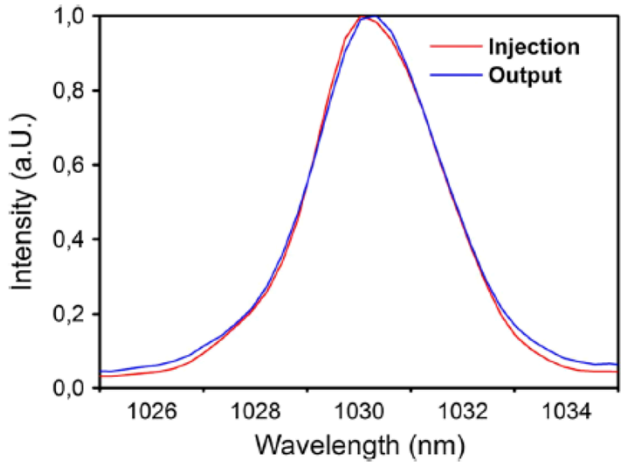

Fig. 10 The output spectrum is 3.1 nm (*blue curve*). It is only reduced by the input spectrum (*red curve*)